

# A Low-Complexity ESPRIT-Based DOA Estimation Method for Co-Prime Linear Arrays

Fenggang Sun <sup>1,2,†</sup>, Bin Gao <sup>2</sup>, Lizhen Chen <sup>1</sup> and Peng Lan <sup>1,\*,†</sup>

<sup>1</sup> College of Information Science and Engineering, Shandong Agricultural University, Tai'an 271018, China; sunfg@sdau.edu.cn (F.S.); lzchen@sdau.edu.cn (L.C.)

<sup>2</sup> College of Communications Engineering, PLA University of Science and Technology, Nanjing 210007, China; feimaxiao123@gmail.com

\* Correspondence: lanpeng@sdau.edu.cn; Tel.: +86-136-6868-2911

† These authors contributed equally to this work.

Academic Editor: Vittorio M. N. Passaro

Received: 7 July 2016; Accepted: 22 August 2016; Published: 25 August 2016

**Abstract:** The problem of direction-of-arrival (DOA) estimation is investigated for co-prime array, where the co-prime array consists of two uniform sparse linear subarrays with extended inter-element spacing. For each sparse subarray, true DOAs are mapped into several equivalent angles impinging on the traditional uniform linear array with half-wavelength spacing. Then, by applying the estimation of signal parameters via rotational invariance technique (ESPRIT), the equivalent DOAs are estimated, and the candidate DOAs are recovered according to the relationship among equivalent and true DOAs. Finally, the true DOAs are estimated by combining the results of the two subarrays. The proposed method achieves a better complexity–performance tradeoff as compared to other existing methods.

**Keywords:** direction of arrival (DOA) estimation; co-prime array; ESPRIT; sparse array; equivalent DOAs

## 1. Introduction

Direction of arrival (DOA) estimation is a crucial problem in various applications, such as radar, sonar, and wireless communications [1]. Various DOA estimation methods have been studied in uniform linear arrays (ULAs), including multiple signal classification (MUSIC) [2] and estimation of signal parameters via rotational invariance technique (ESPRIT) [3]. In [4], a Khatri-Rao product-based real-valued sparse estimation method is proposed. With respect to the random errors of sensor position, a stochastic framework is established to find the probability density function of the DOA-estimates [5]. However, most of the traditional DOA estimation schemes have focused on ULA structure [6], which, in fact, is not an optimal array geometry.

Recently, sparse array geometry has drawn lots of attention due to its high resolution [7–9]. An eigenstructure-based direction-finding algorithm is proposed in [7] for sparse uniform Cartesian arrays. In [8], an ESPRIT-based estimation method is proposed for a sparse array with two different sizes of spatial invariances. Moreover, the literature [9] introduces a novel direction-finding algorithm for a multiscale sensor array, which presents multiple scales of spatial invariance. Except for these sparse structures, the nested arrays [10] and co-prime arrays [11–13] have also attracted great attention. The nested array suffers from the mutual coupling problem due to some closely located sensors, while the co-prime array has less of a mutual coupling effect since sensor elements are sparsely located. Consequently, we consider the co-prime array structure in this paper. Various DOA estimation methods have been proposed for co-prime arrays [14–16]. A projection-like method is proposed in [14] to estimate DOAs by combining the results of the two subarrays. By applying the MUSIC algorithm, a total spectral search-based method (TSS) is proposed in [15], which, however, suffers from the

high complexity caused by the spectral search step. By limiting the searching region to a small sector, a partial spectral search-based method (PSS) is proposed in [16]. It is shown in [16] that the PSS method can achieve almost the same estimation accuracy as TSS, but with a substantially reduced complexity. Further, the PSS method is extended to co-prime planar array structures to estimate two dimensional DOAs in [17]. However, since the complexity is mainly caused by spectral search, the works [16,17] still have a heavy computational burden.

To this end, in this paper, we propose a low-complexity DOA estimation method for co-prime linear arrays. For each subarray of the co-prime array, the true DOAs are mapped into their respective equivalent angles impinging on a traditional ULA with half-wavelength inter-element spacing, which can be obtained by ESPRIT. Then, according to the relationship among true and equivalent DOAs, the candidate DOAs are recovered immediately. Finally, the true DOAs can be uniquely estimated by seeking the common angles recovered by the two subarrays. Simulation results are provided to verify the effectiveness of the proposed method.

## 2. System Model

As shown in Figure 1, we consider a co-prime linear array consisting of two uniform linear subarrays, which are located in the same line. The first subarray has  $M_1$  equal-spaced omnidirectional sensors with inter-element spacing  $M_2\lambda/2$ , while the second has  $M_2$  equal-spaced omnidirectional sensors with inter-element spacing  $M_1\lambda/2$ . Here  $M_1$  and  $M_2$  are co-prime integers, and  $\lambda$  is the wavelength. The two subarrays share the first sensor, and consequently the co-prime array has  $M_1 + M_2 - 1$  sensors.

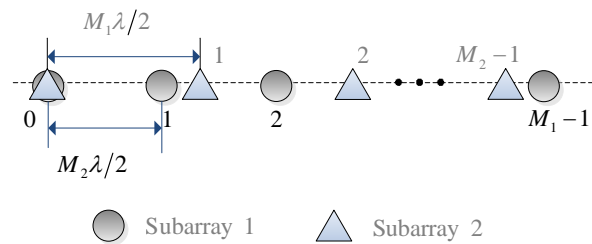


Figure 1. The system model of co-prime linear array.

Assume  $K(K < \min(M_1, M_2))$  uncorrelated narrowband signals impinge on the array. The received signal for the  $i$ th ( $i = 1, 2$ ) subarray at time  $t$  ( $1 \leq t \leq T$ ) is

$$\mathbf{x}_i(t) = \sum_{k=1}^K \mathbf{a}_i(\theta_k) s_k(t) = \mathbf{A}_i \mathbf{s}(t) + \mathbf{n}_i(t) \quad (1)$$

where  $\mathbf{a}_i(\theta_k) = [1, e^{-jM_i\pi \sin(\theta_k)}, \dots, e^{-j(M_i-1)M_i\pi \sin(\theta_k)}]^T$  ( $i + \tilde{i} = 3$ ) is the steering vector for the  $k$ th source  $\theta_k$ ,  $\mathbf{A}_i = [\mathbf{a}_i(\theta_1), \dots, \mathbf{a}_i(\theta_K)]$  is the steering matrix,  $\mathbf{s}(t) = [s_1(t), \dots, s_K(t)]^T$  is the source vector. The components of  $\mathbf{n}_i(t)$  are assumed to be independent and identically distributed additive white Gaussian noise with equal variance in each sensor, and are independent from the sources.  $(\cdot)^T$  denotes the transpose operation.

According to the property of sinusoid function, for each source  $\theta_k$  in the  $i$ th subarray, there exist some particular angles, denoted as  $\theta_{i,k}^{eqv}$ , that satisfy  $\pi \sin \theta_{i,k}^{eqv} = M_i \pi \sin \theta_k + 2n_i \pi$ , where  $n_i$  is an integer. From the definition of  $\mathbf{a}_i(\theta_k)$ , the angle  $\theta_{i,k}^{eqv}$  can be regarded as the equivalent angle for the true  $\theta_k$  impinging on one traditional  $M_i$ -element ULA with half-wavelength spacing, which generates the same steering vector as  $\theta_k$ . The relation between true  $\theta_k$  and its equivalent  $\theta_{i,k}^{eqv}$  is thus given as

$$\sin \theta_{i,k}^{eqv} = M_i \sin \theta_k + 2n_i \quad (2)$$

The signal model in Equation (1) amounts to  $K$  equivalent sources from angles  $\theta_{i,k}^{eqv}$  impinging on a traditional ULA simultaneously. The system model of the  $i$ th subarray of the co-prime array and its equivalent uniform linear array is shown in Figure 2.

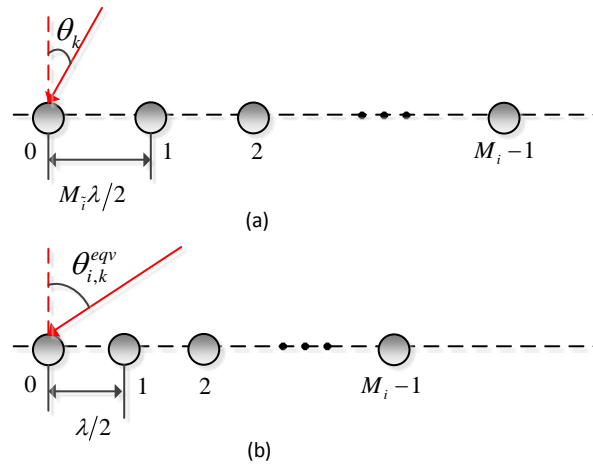


**Figure 2.** The System model of (a) the  $i$ th subarray and (b) its corresponding equivalent array of the co-prime linear array.  $\theta_k$  is the true DOA for the  $k$ th source, and  $\theta_{i,k}^{eqv}$  is the equivalent angle.

### 3. Proposed DOA Estimation Method

The equivalent DOA equals to the true one only when  $M_i = 1$ . In the considered co-prime array, since  $M_i > 1$ , there exist multiple equivalent angles  $\theta_{i,k}^{eqv}$  for each true  $\theta_k$ . The true DOA  $\theta_k$  may be one of the potential equivalent angles recovered by Equation (2), however, which one is the true DOA cannot be determined by each subarray alone. According to the property of coprimeness, the true DOAs can be uniquely estimated by finding the common angles in the two equivalent DOA sets generated by the two subarrays, respectively.

In the following, we aim to find the equivalent DOAs from Equation (1). To avoid the high complexity caused by spectral search, we propose to use the ESPRIT method.

#### 3.1. Proposed Method

The steering matrix  $\mathbf{A}_i$  of the  $i$ th subarray can be rewritten as

$$\mathbf{A}_i = \begin{bmatrix} \mathbf{A}_{i,1} \\ \text{the last row} \end{bmatrix} = \begin{bmatrix} \text{the first row} \\ \mathbf{A}_{i,2} \end{bmatrix} \quad (3)$$

where  $\mathbf{A}_{i,1}$  is the first  $M_i - 1$  rows of  $\mathbf{A}_i$  and  $\mathbf{A}_{i,2}$  is constructed from the last  $M_i - 1$  rows. The relationship between  $\mathbf{A}_{i,1}$  and  $\mathbf{A}_{i,2}$  is

$$\mathbf{A}_{i,2} = \mathbf{A}_{i,1} \mathbf{J} \quad (4)$$

with  $\mathbf{J} = \text{diag} \left( e^{-j\pi \sin \theta_{i,1}^{eqv}}, e^{-j\pi \sin \theta_{i,2}^{eqv}}, \dots, e^{-j\pi \sin \theta_{i,K}^{eqv}} \right)$ .

The eigen-decomposition of the array covariance matrix  $\mathbf{R}_i = E [\mathbf{x}_i(t) \mathbf{x}_i^H(t)]$  of the  $i$ th subarray yields

$$\mathbf{R}_i = \mathbf{U}_{s,i} \mathbf{\Lambda}_s \mathbf{U}_{s,i}^H + \mathbf{U}_{n,i} \mathbf{\Lambda}_n \mathbf{U}_{n,i}^H \quad (5)$$

Here  $E(\cdot)$  and  $(\cdot)^H$  stand for statistical expectation and Hermitian transpose, respectively.  $\mathbf{U}_{s,i}$  and  $\mathbf{U}_{n,i}$  denote the signal- and noise-subspace eigenvectors, respectively.  $\mathbf{\Lambda}_s$  and  $\mathbf{\Lambda}_n$  contain the corresponding eigenvalues.

The signal subspace eigenvector  $\mathbf{U}_{s,i}$  can be similarly partitioned as

$$\mathbf{U}_{s,i} = \begin{bmatrix} \mathbf{U}_{s,i,1} \\ \text{the last row} \end{bmatrix} = \begin{bmatrix} \text{the first row} \\ \mathbf{U}_{s,i,2} \end{bmatrix} \quad (6)$$

where  $\mathbf{U}_{s,i,1} = \mathbf{A}_{i,1}\mathbf{G}$ ,  $\mathbf{U}_{s,i,2} = \mathbf{A}_{i,2}\mathbf{G} = \mathbf{A}_{i,1}\mathbf{J}\mathbf{G}$ , and  $\mathbf{G}$  is a full rank  $K \times K$  matrix. Then, we have

$$\mathbf{G}^{-1}\mathbf{J}\mathbf{G} = \left(\mathbf{U}_{s,i,1}^H \mathbf{U}_{s,i,1}\right)^{-1} \mathbf{U}_{s,i,1}^H \mathbf{U}_{s,i,2} \quad (7)$$

The matrix  $\left(\mathbf{U}_{s,i,1}^H \mathbf{U}_{s,i,1}\right)^{-1} \mathbf{U}_{s,i,1}^H \mathbf{U}_{s,i,2}$  has the same eigenvalues as  $\mathbf{J}$ , while  $\mathbf{J}$  contains the information of the equivalent DOAs. The equivalent DOAs can then be obtained by finding the eigenvalues of the matrix  $\left(\mathbf{U}_{s,i,1}^H \mathbf{U}_{s,i,1}\right)^{-1} \mathbf{U}_{s,i,1}^H \mathbf{U}_{s,i,2}$ . Specifically, assume the  $K$  eigenvalues are denoted as  $d_k (k = 1, 2, \dots, K)$ , the equivalent DOAs of the  $i$ th subarray can be estimated as

$$\hat{\theta}_{i,k}^{eqv} = \arcsin(d_k/\pi) \quad (8)$$

Let  $\hat{\boldsymbol{\theta}}_i^{eqv} = [\hat{\theta}_{i,1}^{eqv}, \hat{\theta}_{i,2}^{eqv}, \dots, \hat{\theta}_{i,K}^{eqv}]$ . The candidate true DOAs can be recovered by Equation (2); i.e.,

$$\hat{\boldsymbol{\theta}}_i^{cand} = \arcsin\left(\frac{1}{M_i} \left(\sin \hat{\boldsymbol{\theta}}_i^{eqv} - 2n_i\right)\right) \quad (9)$$

Here the relationship  $-M_i \leq \left(\sin \hat{\boldsymbol{\theta}}_i^{eqv} - 2n_i\right) \leq M_i$  must hold due to the constraint of the sinusoid function. Hence, the set  $\hat{\boldsymbol{\theta}}_i^{cand}$  contains  $M_i \times K$  candidate DOAs, among which only  $K$  angles are true. According to the coprimeness of  $M_1$  and  $M_2$ , the true DOAs are obtained by finding the  $K$  common angles of the two candidate sets  $\hat{\boldsymbol{\theta}}_1^{cand}$  and  $\hat{\boldsymbol{\theta}}_2^{cand}$ . In practice, due to the effect of noise, the true DOAs are estimated by seeking for the nearest angle pairs.

**Remark 1.** The two candidate sets  $\hat{\boldsymbol{\theta}}_1^{cand}$  and  $\hat{\boldsymbol{\theta}}_2^{cand}$  both contain the  $K$  true DOAs. In particular cases, except for true DOAs, they may have some other common angles (e.g., the candidate DOAs of different sources in different subarrays may have common angles). This may generate more than  $K$  common angles and cause ambiguity as a result. Without loss of generality, we consider  $K = 2$  sources, denoted as  $\theta_1$  and  $\theta_2$ . Let  $\theta_c$  both exist in the candidate set of source 1 in the  $i$ th subarray and the candidate set of source 2 in the  $i$ th subarray; i.e., except for  $\theta_1$  and  $\theta_2$ , they generate another common angle. The relations are denoted as

$$\begin{cases} \sin \theta_c = \sin \theta_1 + \frac{2m_i}{M_i} \\ \sin \theta_c = \sin \theta_2 + \frac{2m_i}{M_i} \end{cases} \quad (10)$$

where  $m_i$  and  $m_i$  are integers. Then we have the relation between  $\theta_1$  and  $\theta_2$  as

$$\sin \theta_1 - \sin \theta_2 = \frac{2m_i}{M_i} - \frac{2m_i}{M_i} \quad (11)$$

It is observed from Equation (11) that only when  $m_i \neq 0$  and  $m_i \neq 0$ , the particular  $(\theta_1, \theta_2)$  pair will generate another common angle. For example, let us consider a co-prime linear array with  $M_1 = 5$  and  $M_2 = 7$  and assume  $\theta_1 = 60.0^\circ$  and  $\theta_2 = 48.7^\circ$ . The two DOAs satisfy the relationship (11). The corresponding ambiguous DOAs generated by each subarray are listed in Table 1. As can be seen, for each source, the estimate of the two subarrays can generate one unique common angle—i.e., the true DOA. However, when the two sources ( $\theta_1 = 60.0^\circ$  and  $\theta_2 = 48.7^\circ$ ) are considered, expect for true

DOAs, the estimate of the two subarrays may generate another two common angles (i.e.,  $-58.0^\circ$  and  $27.8^\circ$ ). This violates the uniqueness and causes ambiguity as a result.

**Table 1.** Two directions of arrival (DOAs) and their corresponding ambiguous DOAs in each subarray.

$\theta_1 = 60.0^\circ$	Subarray 1 with $M_1 = 5$	$-58.0, -34.2, -16.1, 0.51, 17.1, 35.5, 60.0$
	Subarray 2 with $M_2 = 7$	$-47.2, -19.5, 3.8, 27.8, 60.0$
$\theta_2 = 48.7^\circ$	Subarray 1 with $M_1 = 5$	$-74.4, -42.6, -23.1, -6.1, 10.4, 27.8, 48.7$
	Subarray 2 with $M_2 = 7$	$-58.0, -26.7, -2.8, 20.6, 48.7$

However, notice that the incident DOAs are in the continuous range between  $-90^\circ$  and  $90^\circ$ , and only some particular angle pairs  $(\theta_1, \theta_2)$  that satisfy Equation (11) may generate another common ambiguous angle, except for the true DOAs. Specifically, for arbitrarily given  $\theta_1$ , only some discrete angles for  $\theta_2$  follow the relationship Equation (11). Therefore, as compared to the continuous angle range, the number of  $(\theta_1, \theta_2)$  pairs that satisfy Equation (11) is rare. Therefore, the probability of the existence of a different common angle  $\theta_c$  approaches zero and it is consequently a small probability event. Even if this small probability event happens, it can be solved by the entire co-prime linear array. The beamforming-related techniques, such as the classical beamforming approach (CBF) [18] and the Capon's approach (also known as the minimum variance distortionless response, MVDR) [19,20], can be utilized to eliminate the problem. Specifically, the CBF spatial spectrum of the entire co-prime array is

$$P_{CBF} = \mathbf{a}_C^H(\theta) \mathbf{R}_C \mathbf{a}_C(\theta) \quad (12)$$

and the MVDR spatial spectrum is

$$P_{MVDR} = \frac{1}{\mathbf{a}_C^H(\theta) \mathbf{R}_C^{-1} \mathbf{a}_C(\theta)} \quad (13)$$

where  $\mathbf{a}_C(\theta)$  denotes the steering vector with respect to  $\theta$  of the entire co-prime array, and  $\mathbf{R}_C$  is the covariance matrix of the entire co-prime array. By finding the peaks of  $P_{CBF}$  in Equation (12) or  $P_{MVDR}$  in Equation (13) the true DOAs can be estimated, and other ambiguous angles are eliminated. Thus, the ambiguity can be resolved successfully.

**Remark 2.** In general, there exist  $K$  common angles, which are the true DOAs. However, if the incident angles satisfy Equation (11), more than  $K$  common angles can be generated. We need to determine the number  $\hat{K}$  ( $\hat{K} \geq K$ ) of the common angles. Let  $N_1$  and  $N_2$ , respectively, denote the numbers of the relevant angles (including the true and ambiguous angles) for the first and second subarray, and let  $d_i$  denote the absolute value of angle difference, where  $1 \leq i \leq N_1 N_2$ . By sorting  $d_i$  in ascendant order, we have

$$d_1 \leq d_2 \leq \dots \leq d_K \leq \dots \leq d_{N_1 N_2} \quad (14)$$

For common angles of the two subarrays, the angle differences are small (nearly 0), while they become larger for distinct angles. Define a decision variable as

$$D(n) = \frac{d_{n+1} - d_n}{d_n}, n = K, K+1, \dots, N_1 N_2 - 1 \quad (15)$$

Notice that when both  $d_n$  and  $d_{n+1}$  are the differences of common angles or distinct angles, the decision variable will almost keep small. Meanwhile, if  $d_n$  is the difference of common angles

and  $d_{n+1}$  is the difference of distinct angles, the decision variable will become much larger. Thus, the number of common angles can be estimated as

$$\hat{K} = \arg \max_n D(n) \quad (16)$$

When  $\hat{K} > K$ , the true  $K$  DOAs can be distinguished according to Equations (12) and (13).

### 3.2. Complexity Analysis

The complexity of different methods is provided in Table 2. The ESPRIT method with  $M$  sensors and  $K$  sources requires covariance matrix estimation and the eigen-decomposition of both the covariance matrix  $\mathbf{R}_i$  and the matrix  $\left(\mathbf{U}_{s,i,1}^H \mathbf{U}_{s,i,1}\right)^{-1} \mathbf{U}_{s,i,1}^H \mathbf{U}_{s,i,2}$ , and the corresponding complexities are  $\mathcal{O}(M^2T)$ ,  $\mathcal{O}(M^3)$ , and  $\mathcal{O}(3MK^2 + 2K^3)$ , respectively. The resulting complexity of ESPRIT is given as  $\mathcal{O}(M^2T + M^3 + 3MK^2 + 2K^3)$ . The complexity of the proposed method is given similarly. As is shown in Table 2, the complexity of the proposed method is lower than that of ESPRIT.

**Table 2.** Computational complexity comparison.

ESPRIT	$\mathcal{O}(M^2T + M^3 + 3MK^2 + 2K^3)$
PSS [16]	$\mathcal{O}((M_1^2 + M_2^2)T + M_1^3 + M_2^3 + \frac{J}{M_2} M_1(M_1 - K) + \frac{J}{M_1} M_2(M_2 - K))$
Proposed	$\mathcal{O}((M_1^2 + M_2^2)T + M_1^3 + M_2^3 + 3(M_1 + M_2)K^2 + 4K^3)$

Note:  $M = M_1 + M_2 - 1$ ,  $J$  is the number of sampling points. PSS: partial spectral search.

## 4. Results

In this section, we compare the proposed method with PSS [16] in co-prime arrays with  $M_1 = 5$  and  $M_2 = 7$ . For fair comparison, the results of the traditional ESPRIT are also provided for two types of half-wavelength spacing ULAs with  $M_1 + M_2 - 1 = 11$  and  $M_1 M_2 - \min(M_1, M_2) + 1 = 31$  sensors, respectively. The former has the same sensor number as the considered co-prime array, but with less aperture length, denoted as ESPRIT with the same sensor number (ESPRIT-SSN). The latter has the same aperture length, but with more sensor elements, denoted as ESPRIT with the same aperture length (ESPRIT-SAL). The Cramer-Rao bound (CRB) for the co-prime array geometry is also given as a benchmark [21]. The searching grid for PSS is set as  $0.1^\circ$ .

In the first test, we compare the average root mean square error (RMSE) of different methods. Two uncorrelated sources are assumed to impinge on the array from directions  $21^\circ$  and  $41^\circ$ . Figure 3 plots the RMSE performance versus signal-to-noise ratio (SNR) via 200 Monte Carlo simulations with  $T = 200$ . As is shown, under the same sensor number condition, the proposed method outperforms ESPRIT-SSN greatly. With respect to the same aperture length, the proposed method can achieve almost the same estimation accuracy as ESPRIT-SAL. The proposed method is inferior to PSS at low SNR, and gradually exceeds PSS with the increase of SNR. Regarding the complexity, the ESPRIT-SSN, ESPRIT-SAL, PSS, and proposed method requires  $\mathcal{O}(2.57 \times 10^4)$ ,  $\mathcal{O}(2.22 \times 10^5)$ ,  $\mathcal{O}(3.17 \times 10^4)$ , and  $\mathcal{O}(1.55 \times 10^4)$  complexities, respectively. The average running time for the four methods are 5.74 s, 15.60 s, 12.98 s, and 2.66 s. The complexity of the proposed method is lower than that of others, implying that the proposed method needs less memory. Especially, to achieve the same estimation accuracy, the proposed method only requires about 10% computational complexity as compared to ESPRIT-SAL. Therefore, the proposed method can achieve a better complexity–performance tradeoff. Further, Figure 4 depicts the RMSE performance versus snapshot number with SNR = 5 dB. The performance of the proposed method is almost the same as ESPRIT-SAL and is superior to ESPRIT-SSN, but is slightly weaker than that of PSS. However, the performance gap becomes smaller with the increase of snapshot number.

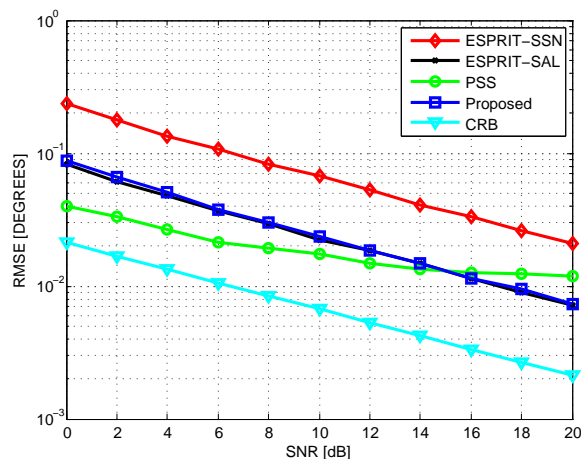


**Figure 3.** Root mean square error (RMSE) vs. signal-to-noise ratio (SNR),  $T = 200$ . CRB: Cramer-Rao bound; ESPRIT: estimation of signal parameters via rotational invariance technique; ESPRIT-SAL: ESPRIT with the same aperture length; ESPRIT-SSN: ESPRIT with the same sensor number.

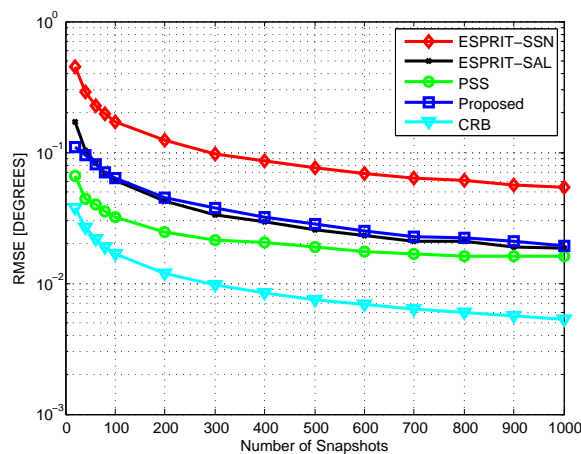


**Figure 4.** RMSE vs. Snapshot Number,  $SNR = 5$  dB.

In the second test, we investigate the resolution probability performance. The two sources are said to be resolvable [22] if both  $|\hat{\theta}_1 - \theta_1|$  and  $|\hat{\theta}_2 - \theta_2|$  are smaller than  $|\theta_1 - \theta_2|/2$ , where  $\theta_k$  and  $\hat{\theta}_k$  ( $k = 1, 2$ ) are the true and estimated DOAs, respectively. We set  $\theta_1 = 20^\circ$  and  $\theta_2 = \theta_1 + \Delta\theta$ , where  $\Delta\theta$  is the control variable. We fix  $SNR = 5$  dB and  $T = 200$  and plot the resolution probability against  $\Delta\theta$  in Figure 5. As can be seen, the resolution ability is enhanced with the increase of  $\Delta\theta$ . The proposed method provides almost the same resolution performance as ESPRIT-SAL, but with substantially reduced complexity. The proposed method provides the best resolution performance as compared to ESPRIT-SSN and PSS.

To eliminate the ambiguity for some particular angle pairs that satisfy Equation (11), we give the ambiguity check results in Table 3. For  $\theta_1 = 48.7^\circ$  and  $60.0^\circ$  as in Table 1, the estimate of two subarrays may generate another two common angles except for true DOAs; i.e.,  $-58.0^\circ$  and  $27.8^\circ$ . We can see that the true DOAs are checked successfully by both CBF and MVDR. Notice that the spatial output powers for MVDR at true DOAs are much higher than that of other common DOAs, thus the MVDR-based check approach has superior resolution ability. However, since an inverse operation of the covariance matrix is required, the MVDR-based approach has a heavy computation burden. Therefore, the CBF-based approach is more feasible when real-time processing is required.



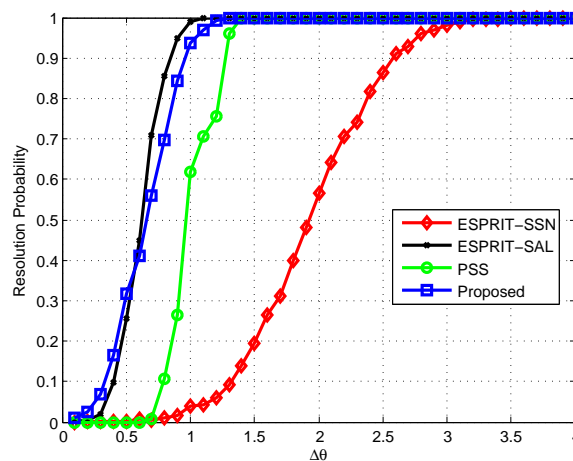


Figure 5. Resolution probability versus  $\Delta\theta$ , with  $\theta_1 = 20^\circ$ ,  $\theta_2 = \theta_1 + \Delta\theta$ .

Table 3. Ambiguity check results of classical beamforming (CBF) and minimum variance distortionless response (MVDR) with  $T = 200$  and  $SNR = 5$  dB.

$\theta$	$-58.0^\circ$	$27.8^\circ$	$48.7^\circ$	$60.0^\circ$
$P_{CBF}   P_{MVDR}$	0.6122   0.0931	0.5974   0.0926	<b>1.3082   0.9561</b>	<b>1.2529   0.9454</b>
True or false	false   false	false   false	true   true	true   true

## 5. Conclusions

In this paper, we have proposed a low-complexity ESPRIT-based DOA estimation method for co-prime arrays. We firstly map the true DOAs into several equivalent angles for each source, which are regarded as the DOAs impinging on traditional uniform linear array. We obtain the equivalent DOAs by ESPRIT and then recover the candidate DOAs according to their relationship. Finally, we uniquely estimate the true DOAs by finding the common angles of the candidate DOAs of the two subarrays. Simulation results show that the proposed method achieves an improved complexity–performance tradeoff in terms of estimation accuracy and resolution ability, as compared to other existing methods.

**Acknowledgments:** This work was supported in part by Shandong Province High School Science & Technology Fund Planning Project (J12LN02), Research Fund for the Doctoral Program of Higher Education of China (20123702120016), and Key Projects in the National Science & Technology Pillar Program during the Twelfth Five-year Plan Period (2011BAD32B02).

**Author Contributions:** Fenggang Sun contributed in the conception and design of the study. Peng Lan wrote and revised the manuscript. Bin Gao carried out the simulation and participated in the design of the study. Lizhen Chen helped perform the analysis with constructive discussions and helped to draft the manuscript. All authors have read and approved the final manuscript.

**Conflicts of Interest:** The authors declare no conflict of interest.

## Abbreviations

DOA	Direction of arrival
ULA	Uniform linear array
ESPRIT	Estimation of signal parameters via rotational invariance technique
MUSIC	Multiple signal classification
TSS	Total spectral search
PSS	Partial spectral search
CBF	Classical beamforming
MVDR	Minimum variance distortionless response
ESPRIT-SSN	ESPRIT with the same sensor number
ESPRIT-SAL	ESPRIT with the same aperture length



CRB      Crame-Rao bound  
 RMSE    Root mean square error  
 SNR      Signal-to-noise ratio

## References

1. Krim, H.; Viberg, M. Two decades of array signal processing research: The parametric approach. *IEEE Signal Process. Mag.* **1996**, *13*, 67–94.
2. Schmidt, R.O. Multiple emitter location and signal parameter estimation. *IEEE Trans. Antennas Propag.* **1986**, *34*, 276–280.
3. Roy, R.; Kailath, T. ESPRIT—Estimation of signal parameters via rotational invariance techniques. *IEEE Trans. Acoust. Speech Signal Process.* **1989**, *37*, 984–995.
4. Chen, T.; Wu, H.; Zhao, Z. The real-valued sparse direction of arrival (DOA) estimation based on the Khatri-Rao product. *Sensors* **2016**, *16*, 693.
5. Inghelbrecht, V.; Verhaevert, J.; van Hecke, T.; Rogier, H. The influence of random element displacement on DOA estimates obtained with (Khatri-Rao-) root-MUSIC. *Sensors* **2014**, *14*, 21258–21280.
6. Ye, Z.; Xu, X. DOA estimation by exploiting the symmetric configuration of uniform linear array. *IEEE Trans. Antennas Propag.* **2007**, *55*, 3716–3720.
7. Zoltowski, M.; Wong, K. Closed-form eigenstructure-based direction finding using arbitrary but identical subarrays on a sparse uniform Cartesian array grid. *IEEE Trans. Signal Process.* **2000**, *48*, 2205–2210.
8. Wong, K.; Zoltowski, M. Direction-finding with sparse rectangular dual-size spatial invariance array. *IEEE Trans. Aerosp. Electron. Syst.* **1998**, *34*, 1320–1336.
9. Miron, S.; Song, Y.; Brie, D.; Wong, K. Multilinear direction finding for sensor-array with multiple scales of invariance. *IEEE Trans. Aerosp. Electron. Syst.* **2015**, *51*, 2057–2070.
10. Pal, P.; Vaidyanathan, P. Nested arrays: A novel approach to array processing with enhanced degrees of freedom. *IEEE Trans. Signal Process.* **2010**, *58*, 4167–4181.
11. Vaidyanathan, P.; Pal, P. Sparse sensing with co-prime samplers and arrays. *IEEE Trans. Signal Process.* **2011**, *59*, 573–586.
12. Shen, Q.; Zhang, Y.; Amin, M.G. Generalized coprime array configurations for direction-of-arrival estimation. *IEEE Trans. Signal Process.* **2015**, *63*, 1377–1390.
13. Pal, P.; Vaidyanathan, P.P. Coprime sampling and the MUSIC algorithm. In Proceedings of the Digital Signal Processing Workshop and IEEE Signal Processing Education Workshop (DSP/SPE), Sedona, AZ, USA, 4–7 January 2011; pp. 289–294.
14. Weng, Z.; Djuric, P. A search-free DOA estimation algorithm for coprime arrays. *Digit. Signal Process.* **2014**, *24*, 27–33.
15. Zhou, C.; Shi, Z.; Gu, Y.; Shen, X. DECOM: DOA estimation with combined MUSIC for coprime array. In Proceedings of the International Conference on Wireless Communications & Signal Processing (WCSP), Hangzhou, China, 24–26 October 2013; pp. 1–5.
16. Sun, F.; Lan, P.; Gao, B. Partial spectral search-based DOA estimation method for co-prime linear arrays. *Electron. Lett.* **2015**, *51*, 2053–2055.
17. Wu, Q.; Sun, F.; Lan, P.; Ding, G.; Zhang, X. Two-dimensional direction-of-arrival estimation for co-prime planar arrays: A partial spectral search approach. *IEEE Sens. J.* **2016**, *16*, 5660–5670.
18. Godara, L.C. Application of antenna arrays to mobile communications. II. Beam-forming and direction-of-arrival considerations. *Proc. IEEE* **1997**, *85*, 1195–1245.
19. Capon, J. High resolution frequency-wavenumber spectrum analysis. *Proc. IEEE* **1969**, *57*, 1408–1418.
20. Benesty, J.; Chen, J.; Huang, Y. A generalized MVDR spectrum. *IEEE Signal Process. Lett.* **2005**, *12*, 827–830.
21. Stoica, P.; Nehorai, A. Performance study of conditional and unconditional direction-of-arrival estimation. *IEEE Trans. Acoust. Speech Signal Process.* **1990**, *38*, 1783–1795.
22. Stoica, P.; Gershman, A.B. Maximum-likelihood DOA estimation by data-supported grid search. *IEEE Signal Process. Lett.* **1999**, *6*, 273–275.

